ACADEMIA ROMÂNĂ
Revue Roumaine de Chimie
http://web.icf.ro/rrch/

Rev. Roum. Chim.,
2018, *63*(7-8), 593-601

Papers

Dedicated to Professor Bogdan C. Simionescu
on the occasion of his 70th anniversary

STUDIES ON THE SORPTION OF LEVOFLOXACIN FROM AQUEOUS SOLUTIONS ONTO NANOHYDROXYAPATITE

Gabriela CIOBANU* and Maria HARJA

"Gheorghe Asachi" Technical University of Iaşi, Faculty of Chemical Engineering and Environmental Protection, Prof. dr. docent Dimitrie Mangeron Rd., no. 73, zip 700050, Iaşi, Roumania

Received July 13, 2017

The present paper involves a study of the adsorption process of the levofloxacin antibiotic from aqueous medium by using the hydroxyapatite nanopowders as adsorbent materials. The monitoring of pH, contact time, adsorbent dosage and drug concentration was carried out in batch adsorption experiments. At pH = 7 and ambient temperature, high levofloxacin removal rates of about 95.24 % and 87.32 % for the uncalcined and calcined nanohydroxyapatites, respectively, were obtained. The kinetic studies indicate that the levofloxacin adsorption onto nanohydroxyapatite samples follows a pseudo-second order kinetic model. High levofloxacin adsorption capacities of 157.09 mg/g and 124.52 mg/g were reported for uncalcined and calcined nanohydroxyapatite samples, respectively. Therefore, hydroxyapatite is an efficient adsorbent for antibiotic pollutants able to protect ecological systems.

INTRODUCTION

Antibiotics are widely used in the human and veterinary medicine, respectively in the therapy of human and animal infections. They are ubiquitous in the worldwide environment, being frequently detected in wastewater, natural water and soils.[1] Antibiotic residues in the environment are considered to be emerging pollutants because the antibiotics and their transformation products may result in the development of antibiotics resistant bacteria or genes in the long-term and have long-term risks to human and ecological health.[2] Therefore, the removal of antibiotics from wastewater becomes an emerging challenge for the global wastewater industry. Among the various technologies for antibiotics removal from water, adsorption is regarded as one of the most prevalent methods.[3-6]

Fluoroquinolones are broad-spectrum antibiotics, effective for both gram-negative and gram-positive the bacteria, which play an important role in the treatment of serious bacterial infections. Fluoroquinolones are divided into 2 groups, based on antimicrobial spectrum and pharmacology: an older group (ciprofloxacin, norfloxacin and ofloxacin) and a newer group (gemifloxacin, levofloxacin and

* Corresponding author: gciobanu03@yahoo.co.uk

moxifloxacin). Fluoroquinolones are widely used in human and veterinary medicine to control bacterial infections, being present in the hospital effluents, but it has also been detected in the farms effluents.[7] Due to their low biodegradability fluoroquinolone drugs are frequently detected in raw water, sediments and sand filtration.[8]

Levofloxacin or levaquin (LV), $C_{18}H_{20}FN_3O_4$, is an antibiotic belonging to the fluoroquinolones group, most used in human and veterinary therapies as antibacterial agent with a broad spectrum of activity against gram-positive and gram-negative bacteria and atypical respiratory pathogens.[9] Since the carbostyril nucleus of the levofloxacin molecule has strong chemical stability, this drug is not fully metabolized in the body and may be excreted, being ultimately discharged into wastewater.[10] Owing to its toxic effects on microbial activity, levofloxacin is often poorly biodegradable in biological treatment systems, being detected as emerging contaminant in aqueous environment.

Hydroxyapatite (HA), $Ca_{10}(PO_4)_6(OH)_2$, a calcium phosphate ceramic, is the most important inorganic component of human hard tissues such as bone, dentine and enamel.[11] Synthetic hydroxyapatite is used in reconstruction surgery, conservative dentistry and dental implantology.[12] Hydroxyapatite has also been investigated as adsorbent for removing many toxic metal ions, dyes, drugs and other contaminants from aqueous solutions.[13-20]

The present work involved a study of the adsorption process of levofloxacin drug from aqueous solutions by hydroxyapatite as adsorbent material. The reason for choosing hydroxyapatite as adsorbent is its non-toxicity, adsorption properties and low-cost material. Besides, the adsorption behaviour of levofloxacin on hydroxyapatite has not yet been studied in the literature until now. Kinetic adsorption experiments were carried out to establish the effect of time on the adsorption process and to determine the removal rate of levofloxacin from solution through adsorption onto hydroxyapatite.

EXPERIMENTAL

1. Materials

Levofloxacin ($C_{18}H_{20}FN_3O_4$, MW = 361.37, CAS Number 100986-85-4, ≥ 98.0% purity) was purchased from Sigma-Aldrich (Germany). Other chemicals, including $Ca(OH)_2$, H_3PO_4 (85 wt.%), NaOH, HCl and ethanol were purchased from Chemical Company (Romania). All reagents were of analytical grade and used without any other purification. Experiments were performed in triply distilled water.

2. Preparation and characterization of nanohydroxyapatite adsorbents

The uncalcined and calcined hydroxyapatite (HA) samples labeled *HA-uc* and *HA-c*, respectively, were prepared by using $Ca(OH)_2$ and H_3PO_4 as raw materials, as presented elsewhere.[21,22] The HA powder was synthesised by the drop-wise addition of a 250 mL solution of $Ca(OH)_2$ (0.1M) to an appropriate amount of H_3PO_4 (0.1M) aqueous solution to achieve predetermined Ca/P atomic ratio of 1.67, under magnetic stirring for 1 h at 60±1 ºC. The pH was continuously monitored and adjusted to 11±0.5 by adding NaOH (1M) aqueous solution. The suspension was aged for 3 h at 60±1 ºC and then filtered and washed with ethanol and triply distilled water. The obtained powder was calcined at 800 ºC in an electrically heated furnace in order to increase its crystallinity.

The phase composition and average crystallite size of the as obtained HA powders were obtained by X-ray diffraction (XRD) with a X'PERT PRO MRD diffractometer (PANalytical, Netherlands) using monochromatic CuKα radiation (λ = 0.15418 nm). The morphology and chemical composition of the samples were studied by scanning electron microscopy (SEM) coupled with energy dispersive X-ray spectroscopy (EDX) with QUANTA 200 3D microscope (FEI, Netherlands). The specific surface areas of the HA powders were evaluated by fitting the Brunauer-Emmett-Teller (BET) equation to the N_2 adsorption isotherms recorded by a Quantachrome Nova 2200e Win2 apparatus. The point of zero charge (pH_{pzc}), defined as the pH where no drift occurs after 48 h, was determined for HA samples by pH drift method.[23]

3. Batch adsorption experiments

All adsorption experiments were carried out using the batch equilibrium technique. Various levofloxacin (LV) solutions with different initial concentrations were prepared by dilution of the LV (1000 mg/L) stock solution. The influence of various parameters such as initial solution pH (2 – 10), HA dose (0.2 – 5 g/L), LV initial concentration (5 – 100 mg/L) and contact time on removal of LV by HA samples (*HA-uc* and *HA-c*) at ambient temperature (20±1 ºC) was investigated by varying one parameter at a time and keeping the remaining other parameters as constant. HCl and NaOH solutions were used to adjust the solution pH. All pH measurements were realized with a Multi-Parameter Consort C831. The concentration of LV in solutions was analysed by UV-Vis Jasco V-550 spectrophotometer at wavelength of maximum adsorption value of LV (λ_{max} = 291 nm). Each experiment was repeated three times and the given results were the average values.

The adsorption capacities (q_t, mg/g) at time t and the removal rate (R, %) were determined using the following equations:

$$q_t = \frac{C_0 - C_t}{m} V \quad (1)$$

$$R = \frac{C_0 - C_t}{C_0} 100 \quad (2)$$

where C_0 and C_t are the initial and t time's concentrations of LV in the solution (mg/L), V is the volume of solution (L), and m is the mass of the adsorbent (g).

Table 1

The adsorption kinetics models

Model	Linear equation	Model parameters	Comments
Pseudo-first order kinetic model	$\log(q_e - q_t) = \log q_e - \frac{k_1}{2.303} \cdot t$ (3)	k_1 = pseudo first-order rate constant (min^{-1})	k_1 and q_e values were calculated from the plot of $\log(q_e - q_t)$ versus t; q_e = adsorption capacity at equilibrium (mg/g)
Pseudo-second order kinetic model	$\frac{t}{q_t} = \frac{1}{k_2 \cdot q_e^2} + \frac{1}{q_e} \cdot t$ (4)	k_2 = pseudo-second order rate constant (g/mg·min)	k_2 and q_e values were calculated from the plot of t/q_t versus t
Intraparticle diffusion model	$q_t = k_{id} \cdot t^{1/2} + c$ (5)	k_{id} = intraparticle diffusion rate constant ($mg/g \cdot min^{0.5}$); c = intercept (mg/g)	k_{id} and c values were calculated from the plot of q_t versus $t^{1/2}$

4. Adsorption kinetics models

The adsorption process order and the rate constant were estimated by applying the pseudo-first order kinetic,[24] pseudo-second order kinetic[25] and intraparticle diffusion[26] models (Table 1), and the model with higher correlation coefficient (R^2) was chosen.

5. Statistical analysis

Each adsorption experiment has been carried out three times and the mean ± SD (standard deviation) has been considered for data analysis to confirm the representative. The analysis was performed by using one-way ANOVA test. Values of $p < 0.05$ were considered statistically significant. The kinetics models fitness was judged by using two non-linear error functions: Chi-square test (χ^2) and Root Mean Square Error (RMSE). The standard equations are as follows:

$$\chi^2 = \sum_{i=1}^{N} \frac{\left(q_{e,exp} - q_{e,calc}\right)^2}{q_{e,calc}} \quad (6)$$

$$\mathrm{RMSE} = \sqrt{\frac{1}{N-2}\sum_{i=1}^{N}\left(q_{e,exp} - q_{e,calc}\right)^2} \quad (7)$$

where $q_{e,exp}$ and $q_{e,calc}$ represent the experimental and calculated values of the adsorption capacity (mg/g) and N is the number of experimental data.

RESULTS AND DISCUSSION

1. Characterization of nanohydroxyapatite adsorbents

The HA nanopowders were prepared and characterized by SEM-EDX, XRD and BET methods, as reported in previous papers.[21,22] The uncalcined and calcined HA samples have hexagonal crystal structure, crystal sizes smaller than 100 nm, and a specific surface area of 316 m^2/g and 139 m^2/g, respectively. Therefore, the uncalcined nanohydroxyapatite would be expected to be able to hold higher amounts of levofloxacin drug than the calcined nanohydroxyapatite. The pH at the point of zero charge (pH_{pzc}) of *HA-uc* and *HA-c* samples was found to be 6.5 and 6.7, respectively. The morphology of the HA samples is shown in SEM micrographs (Fig. 1). The *HA-uc* sample contains needle-like shape crystallites. By contrast, in *HA-c* sample the particles are agglomerated in spherical-like shape aggregates with an average diameter smaller than 200 nm. Also, the micrographs show irregular and porous surfaces with intergranular porosity.

2. Levofloxacin adsorption from solutions

a. Effect of pH

Most quinolone molecules are zwitterionic, based on the presence of a carboxylic acid function and a basic piperazinyl ring in the molecular structure. Both functions are weak and give a good solubility for the quinolones in acidic or basic media. The values for pK_{a1}, correlated with the acid function of carboxyl group, fall in the range 5.33 – 6.53, while the values for pK_{a2}, correlated with the basic function of the piperazinic group, fall in the range 7.57 – 9.33.[27]

Levofloxacin (LV), a new quinolone antibiotic, exists as a zwitterion in the pH range 5.0 – 8.5 and the two pK_a values (5.59 and 7.94) are very close to the isoelectric point (6.77),[28] as shown in Fig. 2. The LEV molecules are primarily cationic (protonated piperazinyl group, H_2LV^+) below pH 5, anionic (deprotonated carboxyl group, LV^-) above pH 8.5, and zwitterionic (or neutral, HLV^o) at pH between its pK_{a1} and pK_{a2} values,[29] as shown in Fig. 3.

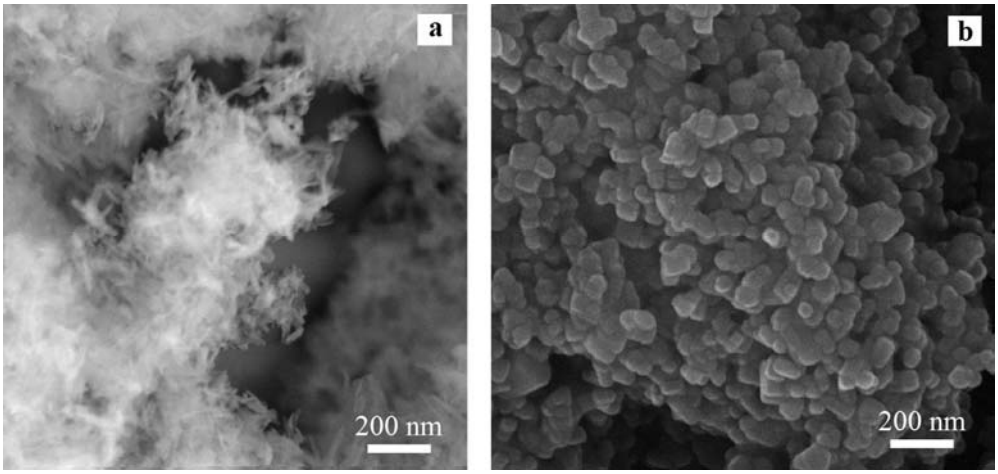

Fig. 1. SEM images of *HA-uc* (a) and *HA-c* (b) hydroxyapatite nanopowders.

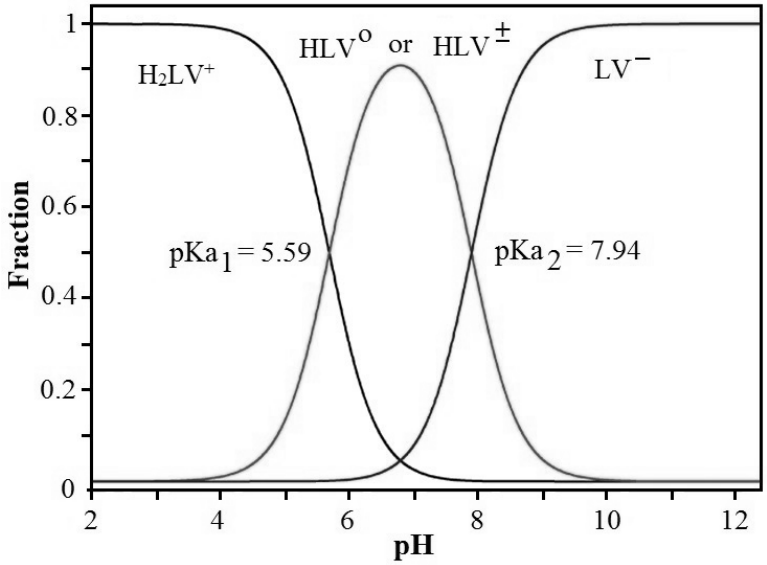

Fig. 2. Levofloxacin distribution as function of pH.

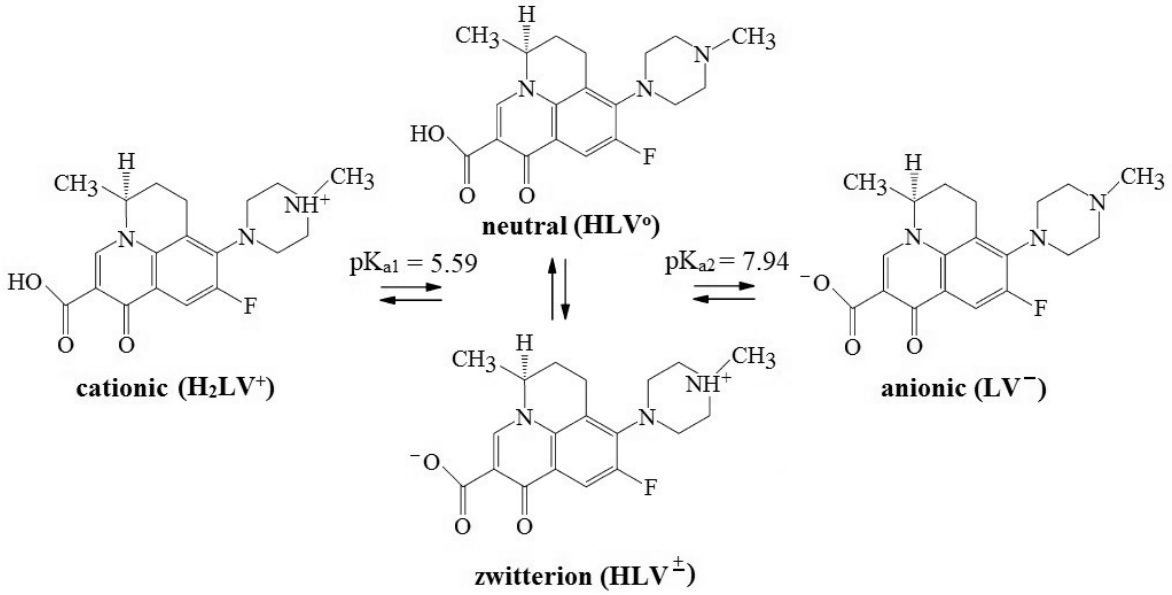

Fig. 3. Molecular structure of Levofloxacin as function of pH.

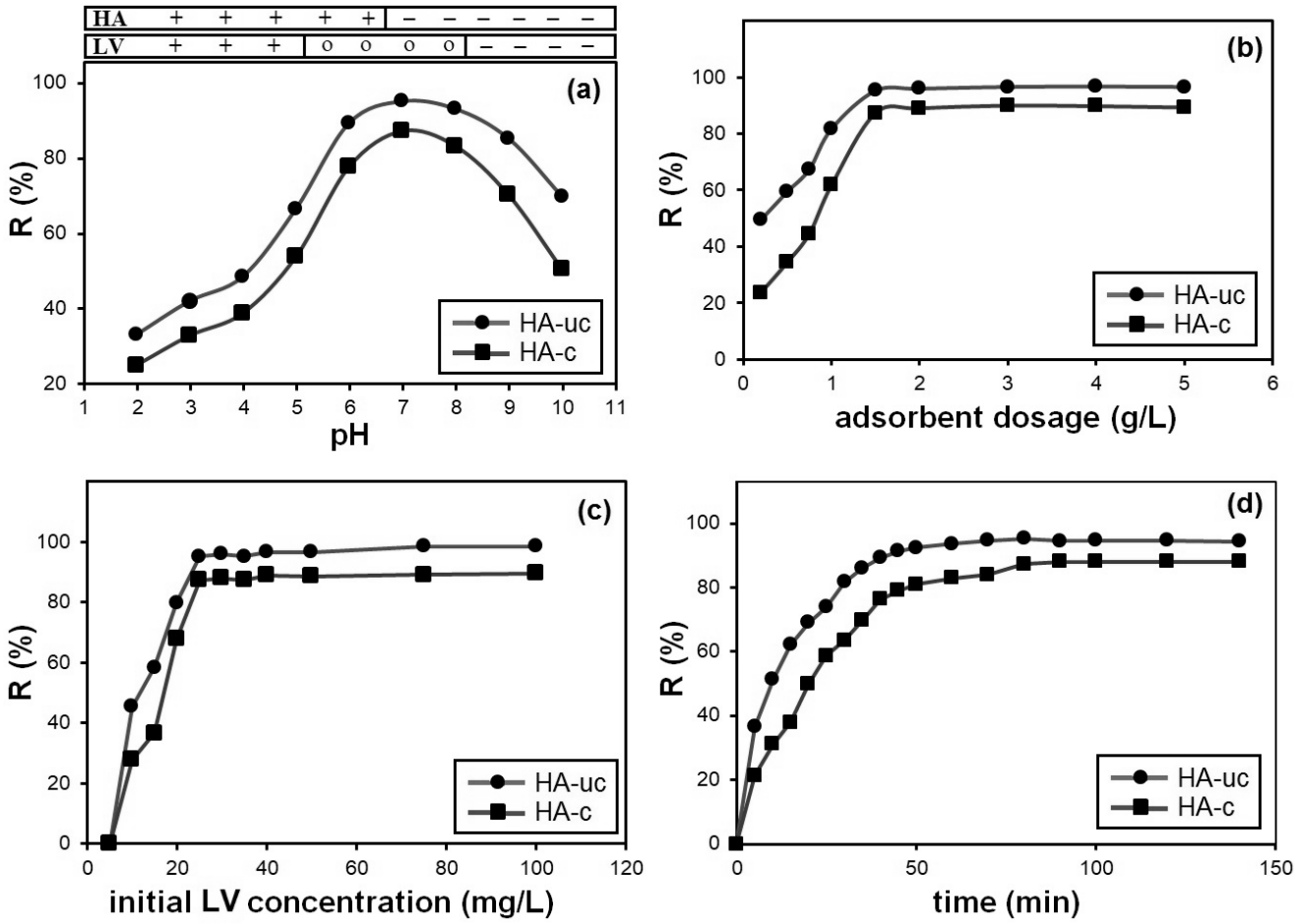

Fig. 4. Effects of pH (a), adsorbent dosage (b), initial LV concentration (c) and contact time (d) on LV adsorption onto *HA-uc* and *HA-c* samples.

Also, the surface charge of HA at different pH in aqueous systems plays a main role in the LV adsorption onto HA. Since the HA surface possesses two different functional groups (≡Ca–OH and ≡P–OH) acting as the active sites, different interactions between these functional groups on the HA surface and the ionic or polar groups of the organic molecules can occur. HA is amphoteric in nature and the H^+ and OH^- are potential-determining ions that develop surface charge on HA. The point of zero charge (pH_{pzc}) of the *HA-uc* and *HA-c* samples was found to be 6.5 and 6.7, respectively, in good agreement with literature data.[30] Hence, the surface of the HA samples becomes positive charged (due to $\equiv CaOH_2^+$ sites) for $pH < pH_{pzc}$ and negative (due to $\equiv OPO_3H^-$ sites) for $pH > pH_{pzc}$. Therefore the pH of the HA suspension plays an important role in deciding the adsorption of the LV molecules.

In order to evaluate the effect of the initial pH on LV adsorption onto *HA-uc* and *HA-c* samples the experiments were carried out within pH range of 2 – 10 keeping all other parameters constant (initial LV concentration 25 mg/L, adsorbent dose 1.5 g/L, contact time 80 min, temperature 20±1 ºC). The results are shown in Fig. 4a. The removal efficiency of LV on both HA samples showed an increase when pH increased from 2 to 7, and then decreased significantly when pH was above 7. At pH 7 and ambient temperature, high LV removal rates of about 95.24 % and 87.32 % for the *HA-uc* and *HA-c* samples, respectively, were obtained. This trend can be understood considering the interactions between LV species and HA surface.

The electrostatic repulsion occurs between LV molecules and HA surfaces at pH < 5 and pH > 8.5 because both are positively and negatively charged, respectively. Over the pH range of 5 – 8.5, the electrostatic interaction may be weakened when hydrophobic interaction is enhanced and dominant due to higher hydrophobicity of zwitterionic LV. Hydroxyapatite may have high adsorption capacity for LV removal with different processes, such as (i) ion-exchange, (ii) surface

complexation and (iii) the formation of insoluble compounds. Our hypothesis is that the sorption mechanism of LV on HA surface at pH = 7 can be established via surface complexation. Physical mechanisms such as van der Waals forces attraction and hydrogen bonding between LV molecules and –OH groups on the surface of HA samples may also contribute to a surface complexation mechanism in LV adsorption. Similar results have been also reported for adsorption of fluoroquinolone antibiotic like LV on activated carbons.[31,32]

b. Effect of adsorbent dosage

The experimental data relating the effect of adsorbent dosage with the removal rate of LV from solution onto HA samples are shown in Fig. 4b. The influence of adsorbent dosage was investigated in the range of 0.2 – 5 g/L adsorbent, keeping all other parameters constant (pH = 7, initial LV concentration 25 mg/L, contact time 80 min, temperature 20±1 ºC). The result showed that, for both hydroxyapatite samples, the LV removal rate increased with increasing adsorbent dosage and the maximum was attained at 1.5 g/L adsorbent dose. This increase in the removal rate with increasing of the adsorbent dose is due to the larger surface and pore volume of adsorbent that is available at higher dose, providing more functional groups and adsorption sites which are favourable for enhancement of the removal efficiency. Therefore, in the following investigations the adsorbent dosage of 1.5 g/L was used.

c. Effect of initial LV concentration

The effect of the solution concentration was studied by varying the initial LV concentration from 5 – 100 mg/L in the test solution, keeping all other parameters constant (pH = 7, adsorbent dose 1.5 g/L, contact time 80 min, temperature 20±1 ºC). The amount of LV adsorbed increased with increase in initial drug concentration tending to saturation at higher drug concentrations (Fig. 4c). The observed increasing of the LV uptake with increasing initial LV concentration by the adsorbents could be due to an increase in interactions between LV and HA, which involves active sites of progressive affinity for the LV species up to saturation point. On the other hand, the removal degree remained constant for LV concentration exceeding 25 mg/L. This value was used in the following investigations.

d. Effect of contact time

The effect of contact time on the removal efficiency of LV by adsorption onto HA samples is presented in Fig. 4d. Adsorption experiments were realised at different contact time, keeping all other parameters constant (pH = 7, initial LV concentration 25 mg/L, adsorbent dose 1.5 g/L, temperature 20±1 ºC). The data shows rapid increase in removal efficiency of LV within the first 20 min, and this may be attributed to a high driving force which accelerates the transfer of LV particles to the adsorbent and the availability of uncovered surface area along with more empty active sites in the initial stage of adsorption. Then, the adsorption gradually increased with increasing contact time until equilibrium was attained, which was considered at 80 min. Therefore, the optimum contact time was selected as 80 min for further experiments.

e. Adsorption kinetics models

In order to determine and interpret the mechanisms of LV adsorption processes over the HA samples and major parameters governing adsorption kinetics, kinetic adsorption data obtained empirically were fitted to the pseudo-first-order, pseudo-second-order, and intra-particle diffusion models shown in Table 1.

Figure 5 shows the fitted plots of adsorption kinetic models for LV by HA samples. The validity of each model is checked by the corresponding correlation coefficients (R^2) as well as the experimental and calculated data summarized in Table 2.

The R^2 values obtained by the pseudo-second order kinetic model (Fig. 5b) were very high, and the calculated adsorption capacity values ($q_{e,calc}$) in Table 2 were in good agreement with the experimental results ($q_{e,exp}$), suggesting the applicability of the pseudo-second order kinetic model to describe the adsorption kinetics data of LV onto HA samples. In this case, the adsorption rate limiting step may be chemisorption and the adsorption of LV occurs probably via surface complexation reactions at specific adsorption sites on HA surface.

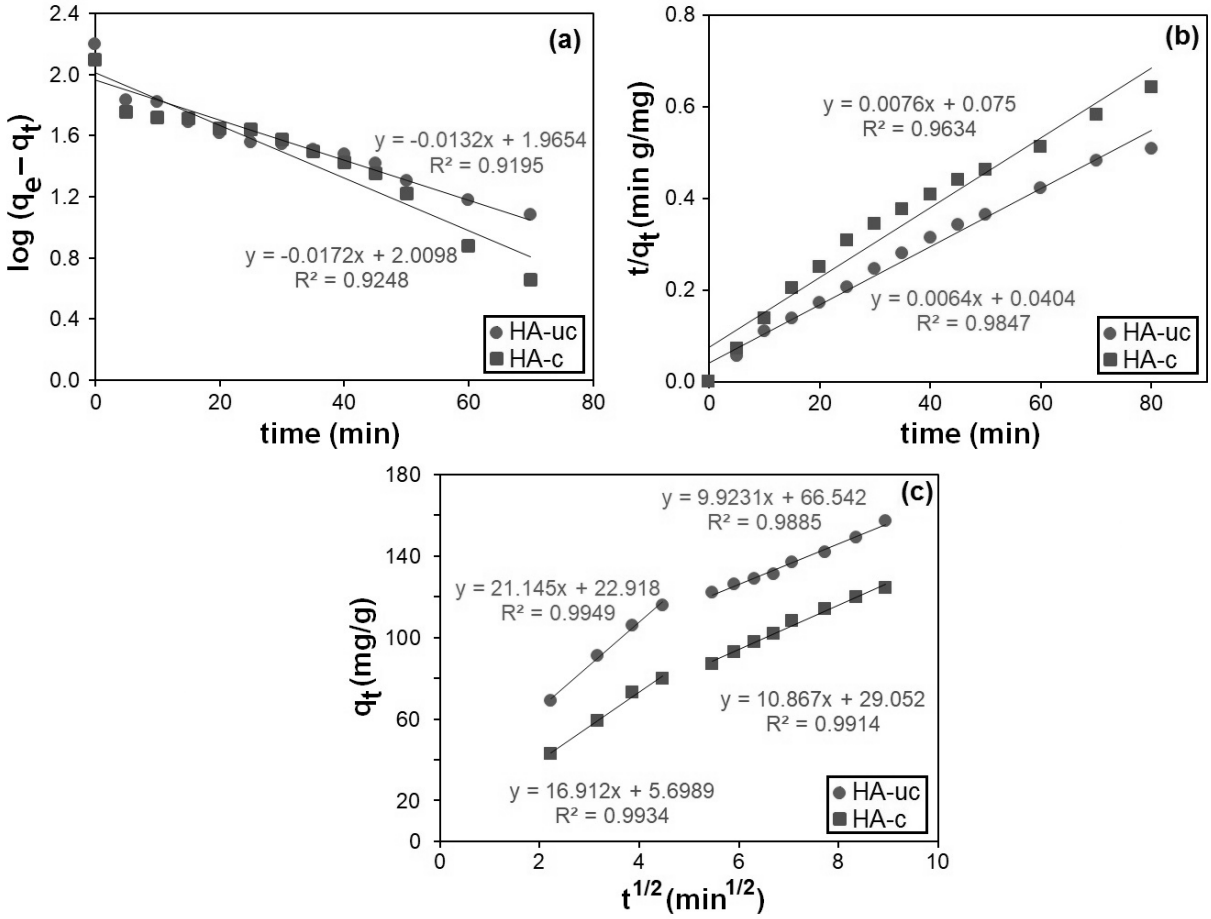

Fig. 5. The pseudo-first order (a), pseudo-second order (b) and intraparticle diffusion (c) kinetic models for LV adsorption onto *HA-uc* and *HA-c* samples.

Table 2

Kinetic parameters for LV adsorption onto HA-uc and HA-c samples

Kinetic model	**Parameter**	**Sample**	
		HA-uc	**HA-c**
	$q_{e,exp}$ (mg/g)	157.09±0.16	124.52±0.23
Pseudo-first order kinetic model	$q_{e,calc}$ (mg/g)	92.34	102.28
	k_1 (min^{-1})	0.0303	0.0396
	R^2	0.9195	0.9248
	χ^2	97.35	57.61
	RMSE	72.54	46.12
Pseudo-second order kinetic model	$q_{e,calc}$ (mg/g)	156.25	131.58
	k_2 (g/mg·min)	0.0010139	0.0007701
	R^2	0.9847	0.9634
	χ^2	1.03	0.34
	RMSE	9.64	5.92

Table 2 (continued)

Intraparticle diffusion model	I	$k_{id(I)}$ (mg/g·min$^{1/2}$)	21.145	16.912
		$c_{(I)}$	22.918	5.698
		$R^2_{(I)}$	0.9949	0.9934
	II	$k_{id(II)}$ (mg/g·min$^{1/2}$)	9.923	10.867
		$c_{(II)}$	66.542	29.052
		$R^2_{(II)}$	0.9885	0.9914

χ^2 = Chi-square, RMSE = Root Mean Square Error; the results are statistically significant ($p < 0.05$).

The validity of the kinetics models for fitting the adsorption data was also assessed by calculating the Chi-square (χ^2) and Root Mean Squared Error (RMSE) values. The lowest values of χ^2 and RMSE indicate the best model fitting and the similarity of the model with the experimental data, respectively.[33] As shown in Table 2, the pseudo-second order kinetic model was found to be statistically significant based on the higher values of the correlation coefficient (R^2) and lower values of χ^2 and RMSE compared to the values obtained for the pseudo-first order kinetic model. Thus the pseudo-second order kinetic model is suitable for modeling the adsorption of LV onto HA samples.

To better understand the mechanism of adsorption, the intraparticle diffusion model was applied. The plot of this model (Fig. 5c) could be evaluated in two linear parts. In the first part (phase I) it occurred LV rapid uptake and the second part (phase II) is associated with the intraparticle diffusion consisting after the accomplishment of external surface coverage by the previous process. The first period is the external surface adsorption or instantaneous diffusion stage, during which a large amount of LV is rapidly adsorbed by the exterior surface of the adsorbent. When the adsorption of exterior surface reaches saturation, the diffusion resistance increases, leading to the decreased diffusion rate, and it is the second period in the adsorption process.

Finally, because of the relatively low-cost of the starting materials and the route used, the resultant hydroxyapatite nanopowders have the potential to be cost-effective adsorbents for the removal of LV from aqueous solutions.

CONCLUSIONS

In the present study the adsorption of the levofloxacin antibiotic from aqueous solution on hydroxyapatite nanopowders was investigated. The adsorption capacity of levofloxacin on uncalcined and calcined hydroxyapatite samples (*HA-uc* and *HA-c*) is up to 157.09 mg/g and 124.52 mg/g, respectively. Removal rates of about 95.24 % and 87.32 % for the *HA-uc* and *HA-c* samples, respectively, were obtained. The kinetic study made evident a fast adsorption process reaching the equilibrium at a contact time of 80 min and pH = 7, for both samples. It was found that the pseudo-second order equation describes in the best way the adsorption kinetics of levofloxacin on calcined and uncalcined hydroxyapatite nanopowders. The levofloxacin adsorption onto hydroxyapatite samples follows the intraparticle (pore) diffusion model. This means that the adsorption process is not only a surface phenomenon, but also a rate-limiting process in the micro- and nanoporous structure of the hydroxyapatite. The obtained results suggest that the levofloxacin adsorption process onto hydroxyapatite samples occurs into two main stages. The first stage involves bulk diffusion of levofloxacin to the adsorbent surface while the second involves intraparticle or pore diffusion processes. The results of the present study are indicative of hydroxyapatite as a new alternative adsorbent for removing the levofloxacin from wastewaters.

REFERENCES

1. K. Kümmerer, *Chemosphere*, **2009**, *75*, 417-434.
2. S. Wang and H. Wang, *Front. Environ. Sci. Eng.*, **2015**, *9*, 565-574.
3. M.B. Ahmed, J.L. Zhou, H.H. Ngo and W. Guo, *Sci. Total Environ.*, **2015**, *532*, 112-126.
4. S. Álvarez-Torrellas, R.S. Ribeiro, H.T. Gomes, G. Ovejero and J. García, *Chem. Eng. J.*, **2016**, *296*, 277-288.
5. F. Yu, Y. Li, S. Han and J. Ma, *Chemosphere*, **2016**, *153*, 365-385.

6. A.M. Bargan, G. Ciobanu, C. Luca, M. Diaconu and I.G. Sandu, *Mater. Plast.*, **2014**, *51*, 167-171.
7. S. García-Segura, J.A. Garrido, R.M. Rodríguez, P.L. Cabot, F. Centellas, C. Arias and E. Brillas, *Water Res.*, **2012**, *46*, 2067–2076.
8. D. Fatta-Kassinos, S. Meric and A. Nikolau, *Anal. Bioanal. Chem.*, **2011**, *399*, 251-275.
9. C. Carbon, *Chemotherapy*, **2001**, *47*, 9-14.
10. I. Ahmad, R. Bano, M.A. Sheraz, S. Ahmed, T. Mirza and S.A. Ansari, *Acta Pharm.*, **2013**, *63*, 223-229.
11. S.V. Dorozhkin, *J. Funct. Biomater.*, **2015**, *6*, 708-832.
12. M. Mucalo, "Hydroxyapatite (HAp) for Biomedical Applications", vol. 95, Elsevier, Woodhead Publishing, Cambridge, 2015.
13. G. Ciobanu and O. Ciobanu, *Desalin. Water Treat.*, **2016**, *57*, 23257-23265.
14. M. Ersan, U.A. Guler, U. Acikel and M. Sarioglu, *Process Saf. Environ. Protect.*, **2015**, *96*, 22-32.
15. G. Ciobanu, S. Ilisei and M. Harja, *Arch. Environ. Prot.*, **2016**, *42*, 3-11.
16. A.C. Queiroz, J.D. Santos, F.J. Monteiro, I.R. Gibson and J.C. Knowles, *Biomaterials*, **2001**, *22*, 1393-1400.
17. G. Ciobanu, M. Harja, L. Rusu, A.M. Mocanu and C. Luca, *Korean J. Chem. Eng.*, **2014**, *31*, 1021-1027.
18. G. Ciobanu, S. Ilisei, M. Harja and C. Luca, *Sci. Adv. Mater.*, **2013**, *5*, 1090-1096.
19. G. Ciobanu, D. Ignat, G. Carja and C. Luca, *Environ. Eng. Manag. J.*, **2009**, *8*, 1347-1350.
20. H. Bouyarmane, I. El Hanbali, M. El Karbane, A. Rami, A. Saoiabi, S. Masse, T. Coradin and A. Laghzizil, *J. Hazard. Mater.*, **2015**, *291*, 38-44.
21. G. Ciobanu, A.M. Bargan and C. Luca, *Ceram. Int.*, **2015**, *41*, 12192-12201.
22. G. Ciobanu, A.M. Bargan and C. Luca, *JOM*, **2015**, *67*, 2534-2542.
23. M.N. Khan and A. Sarwar, *Surf. Rev. Lett.*, **2007**, *14*, 461-469.
24. S. Lagergren, *K. Sven. Vetenskapsakad. Handl.*, **1898**, *24*, 1-39.
25. Y.S. Ho and G. McKay, *Chem. Eng. J.*, **1998**, *70*, 115-124.
26. W.J. Weber jr. and J.C. Morris, *J. Sanit. Eng. Div.*, **1963**, *89*, 31-60.
27. V. Uivarosi, *Molecules*, **2013**, *18*, 11153-11197.
28. B.K. Singh, D.V. Parwate and S.K. Shukla, *E-J. Chem.*, **2009**, *6*, 377-384.
29. M.T. Montero, D. Saiz, R. Sitges, J.L. Vazquez and J.H. Borrell, *Int. J. Pharm.*, **1996**, *138*, 113-120.
30. L.C. Bell, A.M. Posner and J.P. Quirk, *J. Colloid Interface Sci.*, **1973**, *42*, 250-261.
31. M.J. Ahmed and S.K. Theydan, *J. Taiwan Inst. Chem. Eng.*, **2014**, *45*, 219-226.
32. T.M. Darweesh and M.J. Ahmed, *Environ. Toxicol. Pharmacol.*, **2017**, *50*, 159-166.
33. Y.S. Ho and A.E. Ofomaja, *J. Hazard. Mater.*, **2006**, *129*, 137-142.